

Coulomb dissociation studies for reactions in steady and explosive hydrogen burning

T. Motobayashi

Department of Physics, Rikkyo University, Tokyo, Japan

Received: 1 May 2001

Abstract. Radiative capture processes in steady and explosive hydrogen burning sometimes involve unstable nuclei. The Coulomb dissociation method has been used to determine the cross-sections of such reactions indirectly with intermediate-energy RI beams. Recent studies on reactions in the pp chain, hot pp chain and CNO cycle are discussed.

PACS. 25.60.-t Reactions induced by unstable nuclei – 25.70.De Coulomb excitation – 26.65.+t Solar neutrinos

1 Coulomb dissociation with RI beams

Coulomb dissociation can be used to study radiative capture processes of astrophysical interest. This idea was first proposed by Baur, Bertulani and Rebel [1] based on the semi-classical virtual photon theory. The residual nucleus B of the $A(x,\gamma)B$ process bombards a high- Z target, and is Coulomb excited to an unbound state that decays to the $A+x$ channel. Since the process is regarded as absorption of a virtual photon, *i.e.* $B(\gamma,x)A$, the radiative-capture (the inverse of the photoabsorption) cross-section can be extracted from the dissociation yield. Topical reviews were given by Baur and Rebel [2]. In addition to the advantage of the possibility to use thick targets, the Coulomb dissociation enhances the original capture cross-section by a large factor. This is due to the large virtual-photon number and the phase space factor. The two factors can be in the order of 100 to 1000 in the actual case of ${}^8\text{B}$ dissociation, and this large factor enables experiments with RI beams the intensities of which are much weaker than stable beams.

After pioneering studies for the stable Li isotopes, ${}^6\text{Li} \rightarrow \alpha + d$ and ${}^7\text{Li} \rightarrow \alpha + t$, mostly at around $E_{\text{in}} = 10$ MeV per nucleon [3–8], the first Coulomb dissociation experiments with radioactive beams were made for the ${}^{208}\text{Pb}({}^{14}\text{O}, {}^{13}\text{Np}){}^{208}\text{Pb}$ reaction at higher incident energies of 87.5 [9] and 70 MeV/nucleon [10]. The results demonstrates the usefulness of the method, and stimulated further studies such as ${}^{12}\text{N} \rightarrow {}^{11}\text{C} + p$ [11] and ${}^8\text{B} \rightarrow {}^7\text{Be} + p$ [12–18]. We report here recent experimental studies of Coulomb dissociation with RI beams to investigate several radiative capture reactions which are involved in steady and explosive hydrogen burning in stars.

2 Steady burning

Most of the reactions in the steady hydrogen burning can be studied with the combination of a stable target and

a proton beam. However, in some cases the use of RI beams is useful to study the behaviors of low-energy cross-sections of (p,γ) processes.

2.1 Coulomb dissociation of ${}^8\text{B}$

2.1.1 Solar neutrino and the ${}^7\text{Be}(p,\gamma){}^8\text{B}$ reaction

The ${}^7\text{Be}(p,\gamma){}^8\text{B}$ reaction at low energies is the source of high-energy solar neutrinos. The β^+ decay ${}^8\text{B} \rightarrow {}^8\text{Be}(2^+) + e^+ + \nu$ has a high end-point energy of about 14 MeV. (Note that the 2^+ state of ${}^8\text{B}$ is a broad resonance with $\Gamma = 1.5$ MeV.) The flux of these neutrinos measured on the earth is systematically lower than expected. This puzzle is called solar-neutrino problem, and has been discussed intensively since the first terrestrial neutrino measurement was reported by Davis *et al.* in the '60s [19]. The measurement is still continuing, and the most recent result quoted the flux of 2.56 ± 0.23 SNU [20], where SNU abbreviates Solar-Neutrino Unit (10^{-36} interactions per atom per second in the detector material). This is only $34 \pm 6\%$ of the prediction by the standard solar model of Bahcall, Pinsonneault and Basu [21]. Another solar-neutrino measurement at Kamioka mine also observes the ${}^8\text{B}$ neutrinos. The measured flux in their latest report is $48 \pm 9\%$ [22] of the prediction of the model of ref. [21]. Since the flux of the solar neutrino originating from ${}^8\text{B}$ depends directly on the ${}^7\text{Be}(p,\gamma){}^8\text{B}$ cross-section at around 20 keV, the Gamow energy or the effective burning energy in the sun, its experimental information for the low-energy cross-section is of crucial importance in predicting the high-energy neutrino flux.

New solar-neutrino measurements with gallium have a low threshold energy, so that the measured flux contains about 50% contribution from the $p + p \rightarrow D + e^+ + \nu$ and $p + p + e^- \rightarrow D + \nu$ processes. The experiments called SAGE [23], Gallex [24] and GNO [25] observed neutrinos of about 75 SNU, which is lower than the prediction

128^{+9}_7 SNU [21]. In the MSW model [26], the “matter-induced neutrino oscillation” reduces the neutrino flux through disappearance of electron neutrinos through the mixing of a different generation, μ or τ , of neutrino. In the model, the mass difference and mixing angle for the two different neutrinos are extracted by combining the measured and predicted neutrino flux for experiments with different threshold conditions. Therefore, accurate determination of the cross-section for solar reaction including ${}^7\text{Be}(p,\gamma){}^8\text{B}$ becomes even more important after the results of the gallium experiments [23–25] were reported.

For reactions at low energies, the astrophysical S -factor is often used instead of the cross-section σ as, $\sigma(E) = SE \exp[-2\pi\eta]$, where the term $E \exp[-2\pi\eta]$ accounts for the steep energy dependence of $\sigma(E)$ due to the Coulomb penetration in S -wave, where η denotes the Sommerfeld parameter $e^2 Z_1 Z_2 / \hbar v$. Since the first experimental study by Kavanagh was reported in 1960 [27], many experiments have been performed for accurate measurements of the S_{17} -factor for the ${}^7\text{Be}(p,\gamma){}^8\text{B}$ reaction directly [28–35]. The most recent recommendation for the zero-energy S_{17} -factor is given in ref. [36] as $S_{17}(0) = 19^{+4}_{-2}$ eV b, which is obtained by evaluating the direct capture data up to 1998.

Since ${}^7\text{Be}$ is an unstable isotope with 53 day half-life, most of the direct (p,γ) experiments employ a radioactive target. (Note that the experiment described in ref. [35] uses a ${}^7\text{Be}$ beam and a hydrogen target.) This requires special attention in the determination of the beam target luminosity. Attempts to employ the Coulomb dissociation method have also been made for determination of S_{17} hoping that the measurements are independent of the difficulties associated with the direct measurements.

2.1.2 Experiments at 50 MeV/nucleon

The first ${}^8\text{B}$ dissociation experiment was performed at RIKEN [12,13]. Radioactive ${}^8\text{B}$ nuclei were produced by the ${}^{12}\text{C} + {}^9\text{Be}$ interaction at 92 MeV/nucleon, and were analyzed by the RIPS fragment separator [37]. The ${}^8\text{B}$ beam energy in the center of the target, 50 mg/cm² ${}^{208}\text{Pb}$, was 46.5 MeV/nucleon. A ΔE - E plastic scintillator hodoscope detected the outgoing particles of the Coulomb dissociation, ${}^7\text{Be}$ and p, in coincidence. Their energies were determined from their time-of-flight. The particle identification was made by the ΔE - E method, and the scattering angles were determined by the positions in the hodoscope. The p- ${}^7\text{Be}$ relative energies were constructed from these observable. The coincidence yield was then converted to the ${}^7\text{Be}(p,\gamma){}^8\text{B}$ cross-section with the help of a Monte Carlo simulation calculation which included the detection efficiency and the theoretical Coulomb dissociation cross-sections calculated by the distorted-wave theory.

The second RIKEN experiment at 51.9 MeV/nucleon [14,15] used a stack of sixty NaI(Tl) scintillators called DALI in addition to the hodoscope. It measured the de-excitation γ -rays from the first excited state of ${}^7\text{Be}$ at 429 keV populated in the dissociation process. The contribution from this process was measured to be about

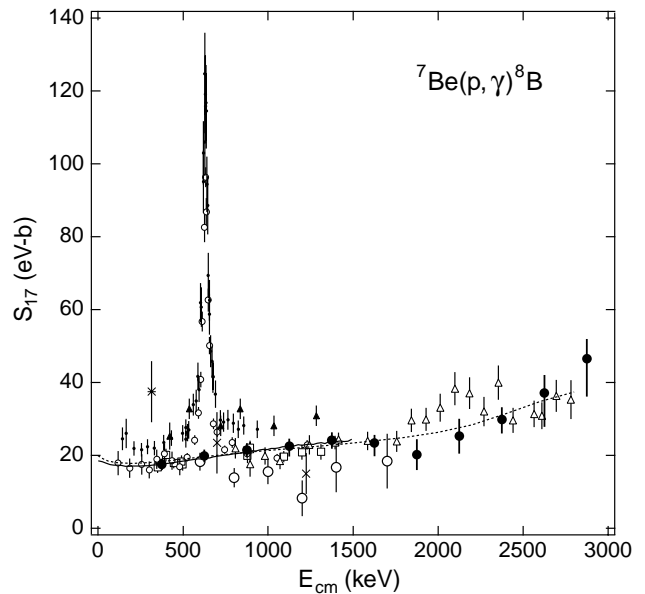


Fig. 1. Astrophysical S -factors for the ${}^7\text{Be}(p,\gamma){}^8\text{B}$ reaction extracted from the first (large open circles) and second (large solid circles) experiments at RIKEN. Direct (p,γ) data are also shown. The solid and dashed curves represent the fits to the data from the second Coulomb dissociation experiment with the theoretical energy dependence of Barker and Spear [38] and that of Descouvemont and Baye [39], respectively.

5% of the Coulomb dissociation yield as an average for $500 \text{ keV} < E_{\text{rel}} < 3 \text{ MeV}$.

In fig. 1 the astrophysical S_{17} -factors obtained in the first and second experiments are shown together with the results from direct (p,γ) measurements. The Coulomb dissociation data are consistent within errors with the direct-capture results by Vaughn *et al.* [30], Filippone *et al.* [32] and Hammache *et al.* [33] which give lower S_{17} -factors than the ones by Parker [28] and Kavanagh [29]. The S -factor extrapolated to zero energy, $S_{17}(0)$, for the first experiment is 16.7 ± 3.2 eV b, and the second experiment with better accuracy gives 18.9 ± 1.8 eV b [15]. The latter is within the range of the recommendation 19^{+4}_{-2} eV b [36].

2.1.3 GSI experiment at 254 MeV/nucleon

Another experiment at a higher incident energy of 254 MeV/nucleon was performed at GSI [16]. A ${}^8\text{B}$ beam was produced by fragmentation of a 350 MeV/nucleon ${}^{12}\text{C}$ beam from the SIS synchrotron. The beam was isotopically separated in the fragment separator FRS [40] and transported to the target position of the spectrometer KaoS [41]. The reaction products were momentum analyzed, and detected in coincidence at the KaoS focal plane. The scattering angles of the fragments were determined by silicon microstrip detectors set between the target and the spectrometer. The result $S_{17}(0) = 20.6 \pm 1.2 \pm 1.0$ eV b agrees with the RIKEN data and hence the direct-capture data with lower S -factors.

2.1.4 E2 component

The ${}^7\text{Be}(p,\gamma){}^8\text{B}$ reaction is dominated by $E1$ γ emission through continuum states. The $E2$ amplitude is very small, but is enhanced in the Coulomb dissociation process because of its much higher sensitivity compared with the $E1$ transition as demonstrated in fig. 2, where the virtual photon intensities are plotted against the incident energy. On the other hand, the $M1$ transition is suppressed in the Coulomb dissociation, while it might have a certain contribution in the direct (p,γ) process.

The second RIKEN experiment [14] was aimed at measuring the $E2$ component from the precise angular distribution of θ_8 , the scattering angle of the p - ${}^7\text{Be}$ center-of-mass. In the vicinity of the grazing angle, the $E1$ cross-section decreases, whereas the one for $E2$ stays almost constant. Therefore, the $E2$ contribution may be observed at large angles even if it is small. As shown in fig. 3, the results suggest that the mixture of the $E2$ component should be negligibly small. It should be pointed out that the analysis includes the nuclear component with the angular-momentum transfer $\ell = 2$, which will be discussed later.

For the same purpose, the extraction of $E2$ component, the parallel-momentum distribution of the ${}^7\text{Be}$ fragment from the Coulomb dissociation of ${}^8\text{B}$ has been measured at MSU [42]. They observed asymmetric peak shapes that are interpreted as an interference between $E1$ and $E2$ amplitudes. The extracted $E2$ component is in the same order as those predicted by nuclear structure models for ${}^8\text{B}$. This conclusion is in contradiction to the angular distribution measurement, requiring further studies.

2.1.5 Higher-order processes

The post acceleration is one of the effects of higher-order processes. It is expected to be small owing to the

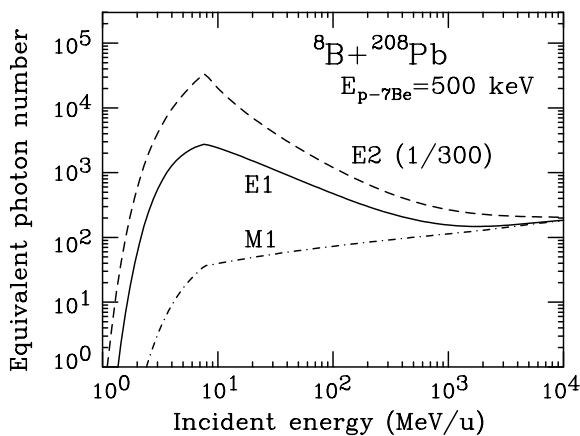


Fig. 2. Number of virtual photon plotted as a function of the incident energy of the ${}^8\text{B} + {}^{208}\text{Pb}$ interaction. The p - ${}^7\text{Be}$ relative energy in the final state is assumed to be 500 keV. The solid, dashed and dash-dotted curves represent, respectively, the $E1$, $E2$ (scaled by $1/300$) and $M1$ transitions.

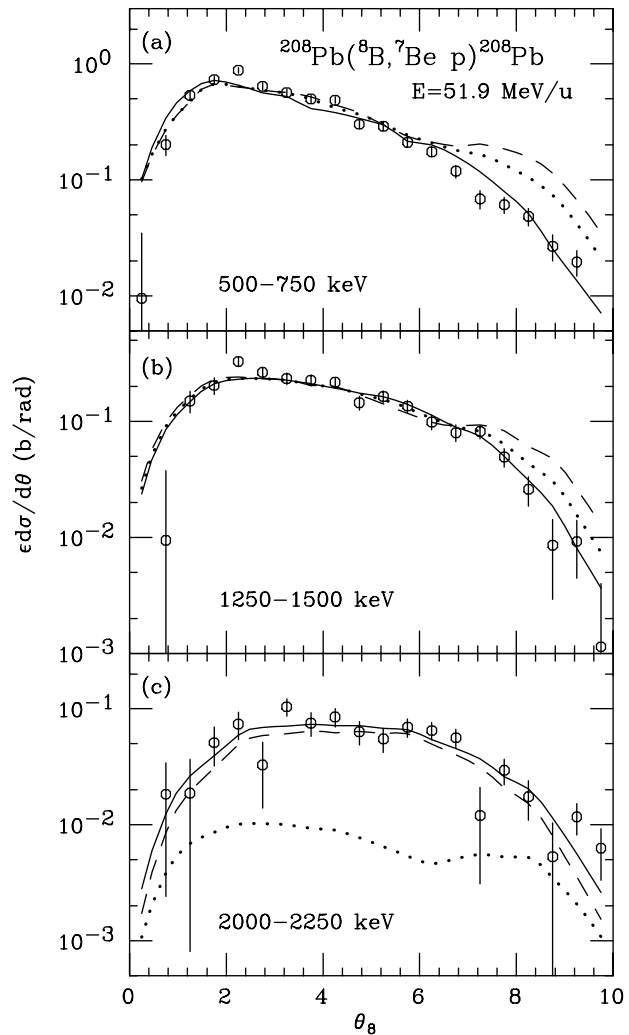


Fig. 3. Angular distributions for the Coulomb dissociation of ${}^8\text{B}$ measured at 51.9 MeV/nucleon for three relative energy bins. The best fits result in pure $E1$ transitions (solid curves in (a) and (b)). Dashed and dotted curves in (a) and (b) correspond respectively to two different models for the ${}^7\text{Be}(p,\gamma){}^8\text{B}$ process which are normalized to the data by fixing the ratios between the $\ell = 1$ and $\ell = 2$ components to the theoretical predictions. For $\ell = 2$, the nuclear excitation amplitudes are included together with the $E2$ Coulomb amplitude, whereas the $\ell = 1$ nuclear amplitudes are not included, because they are expected to be negligibly small.

special situation for ${}^8\text{B}$, where the proton binding energy is only 137 keV. Trajectories very far from the target contribute to excite the continuum state of ${}^8\text{B}$, because a low-energy virtual photon is responsible for the excitation. Various theoretical investigations with semi-classical treatment [43], sudden approximation [44,45], time-dependent Schrödinger equation approach [46,47], and coupled-channel method [48] mostly support the above picture. They predict corrections to the extracted S_{17} -factors smaller than a few % for the conditions of the RIKEN experiments.

The higher-order effects are reduced as the collision time gets shorter or the incident energy gets higher. In

this respect, the agreement between the results obtained at the different energies (50 MeV/nucleon at RIKEN, 80 MeV/nucleon at MSU and 250 MeV/nucleon at GSI) might indicate the dominance of the first-order process. However, at much lower incident energies, the higher-order process might be important. This has been demonstrated by experiments at Notre Dame University [49,50]. A low-energy secondary beam of ^8B at 3.2 MeV/nucleon bombarded a ^{58}Ni target, and the ^7Be fragments were detected. The primary aim of the experiment was to extract the $E2$ component with the help of the intense $E2$ virtual photons as indicated in fig. 2. However, the angular distribution taken in the range from 20° to 70° is quite inconsistent with first-order theories, whereas calculations including higher-order effects [51,52] well reproduced the data. This demonstrates the importance of the higher-order effects at sub-Coulomb energies.

2.1.6 Nuclear contribution

For the ^8B dissociation in its $E1$ component, Bertulani made a calculation based on a one-body potential model for the nuclear structure of ^8B [43], and found that the $\ell = 1$ nuclear-excitation cross-section is only in the order of 1% of the $E1$ cross-section. The same conclusion was obtained by Shyam, Thompson and Dutt-Mazumder [53].

However, the situation changes for $E2$ transitions. The $\ell = 2$ nuclear and $E2$ amplitudes are expected to be in the same order. Figure 4 shows a comparison between the angle-integrated Coulomb and nuclear cross-sections for $\ell = 1$ and $\ell = 2$. They are calculated quantum mechanically. Collective deformation model is used for constructing the transition form factors with a common deformation length. As shown in the figure, the nuclear contribution is important for light nuclei as ^8B .

Therefore, the nuclear excitation with $\ell = 2$ affects the Coulomb dissociation results, if the $E2$ mixture is sizable. For that case, full microscopic calculations are desirable, because the calculated nuclear breakup cross-section

is sensitive to the proton wave function in ^8B and the simple collective-deformation model is not enough for accurate predictions.

2.1.7 Summary of the ^8B dissociation studies

The results discussed above indicate that the S_{17} -factors extracted from the Coulomb dissociation studies are not far from the one recommended and used in solar-model calculations. This gives a support to the recommended reaction rate of the $^7\text{Be}(p,\gamma)^8\text{B}$ reaction used in solar models. However, for more accurate determination of the S_{17} -factor by the Coulomb dissociation, detailed investigation on the reaction mechanism is required. Possible corrections due to the mixture of $E2$ and nuclear components and higher-order processes should be carefully evaluated.

2.2 Coulomb excitation of ^{15}O

Coulomb dissociation is regarded as inelastic excitation to unbound states. The one to bound state is Coulomb excitation, which is also useful in evaluating astrophysical reaction rates. The low-energy behavior of the process $^{14}\text{N}(p,\gamma)^{15}\text{O}$, a key reaction of the CNO cycle hydrogen burning in stars, is not well understood. Especially, a significant contribution to the ground-state capture from the resonance at 504 keV below the $p + ^{14}\text{N}$ threshold, which corresponds to the $3/2^+$ state at 6.793 MeV in ^{15}O , has been pointed out [54]. The measurement for the Coulomb excitation of ^{15}O to this state provides the electromagnetic width Γ_γ , and hence may clarify the role of this sub-threshold state for the $^{14}\text{N}(p,\gamma)^{15}\text{O}$ cross-section at low energies.

An ^{15}O beam was focused onto a 1480 mg/cm^2 ^{208}Pb target at 300–400 kcps. The average beam energy was 85 MeV/nucleon in the middle of the target. The plastic-scintillator hodoscope discussed in subsubsection 2.1.2 detected the scattered ^{15}O . The DALI NaI(Tl) scintillator array measured γ -rays. The Doppler effects were corrected by the γ -ray emission angle determined for each crystal.

In the Doppler-corrected γ spectrum measured in coincidence with ^{15}O , no distinct peak was observed at 6.793 MeV. From this observation, the larger value $\Gamma_\gamma = 6.3 \text{ eV}$ [54] was excluded by a comparison of the simulated yield with the data, whereas the lower estimate of 0.87 eV [55] was compatible with the data. Thus, the present results suggest that $\Gamma_\gamma \leq 1 \text{ eV}$, pointing to only a minor effect of the 6.793 MeV state on the low-energy $^{14}\text{N}(p,\gamma)^{15}\text{O}$ cross-section.

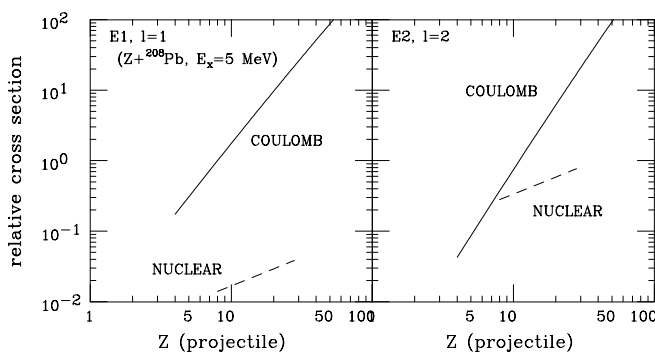


Fig. 4. Atomic number dependence of the Coulomb and nuclear excitation cross-sections for the process, $Z + ^{208}\text{Pb} \rightarrow Z^* + ^{208}\text{Pb}$, where a nucleus Z with atomic number Z is excited to its 5 MeV state. The incident energy is set to be 70 MeV/nucleon. The left panel corresponds to $\ell = 1$ ($E1$) and the right panel to $\ell = 2$ ($E2$) transition.

3 Explosive burning

In the so-called explosive situation, which is expected to be realized in novae, X-ray bursts, and so on, the temperature and density are very high so that even short-lived nuclei can contribute to the nuclear burning. It is almost

impossible to study directly the reactions in such scenarios. The Coulomb dissociation is one of the method that has an access to these reactions. We performed experiments to determine the $E1$ strength of excited levels in ^{12}N and ^{13}O , which dominate the low-energy cross-sections of the $^{11}\text{C}(p,\gamma)^{12}\text{N}$ and $^{12}\text{N}(p,\gamma)^{13}\text{O}$ reactions, respectively, important processes in the hot pp-mode burning in hydrogen-rich massive objects [56]. For the present ^{12}N dissociation experiment, the relative-energy resolution is improved compared with the earlier experiment at GANIL [11]. For ^{13}O , only one resonant state is known at the p- ^{12}N center-of-mass energy $E_{\text{cm}} = 1.23$ MeV corresponding to the excited state at $E_{\text{ex}} = 2.75$ MeV, whose spin is not fully confirmed.

The experimental setup was essentially the same as the one used in the ^8B breakup experiments. Radioactive beams of 77.0 MeV/nucleon ^{12}N and 83.5 MeV/nucleon ^{13}O bombarded 30 and 55 mg/cm 2 ^{208}Pb targets, respectively. The observed p- ^{11}C relative-energy spectrum for the ^{12}N dissociation experiment could be decomposed by three contributions: two resonances at $E_{\text{cm}} = 0.359$ MeV and 0.589 MeV and a direct proton capture. The $E1$ γ width of the second resonance at 0.589 MeV (2^- state at $E_{\text{ex}} = 1.19$ MeV) was extracted to be $\Gamma_\gamma \approx 20$ meV. This is in between two different predictions by Wiescher *et al.* [57] (2 meV) and Descouvemont and Baraffe [58] (140 meV), and disagrees with the results of the GANIL experiment ($6_{-3.5}^{+7}$ meV) [11].

For the ^{13}O dissociation, the experimental relative-energy spectrum exhibits a broad bump at $E_{\text{rel}} \approx 0.8$ MeV. It might contain some extra strength in addition to the $E1$ strength to the resonance at $E_{\text{ex}} = 2.75$ MeV. The sum of the observed strength is much higher than expected in ref. [57], but is similar to the recent large-scale shell model prediction [59].

4 Test of the method

Coulomb dissociation measurements were performed for the processes $^{13}\text{N} \rightarrow ^{12}\text{C} + p$ and $^{14}\text{O} \rightarrow ^{13}\text{N} + p$ in the field of ^{208}Pb via the lowest $E1$ resonances in ^{13}N ($1/2^+$; $E_{\text{ex}} = 2.37$ MeV) and ^{14}O (1^- ; $E_{\text{ex}} = 5.17$ MeV), respectively. The earlier results of the ^{14}O dissociation at RIKEN [9] and GANIL [10] agreed with the direct measurement performed at Louvain-La-Neuve [60]. The RIKEN experiment [9] measured also the ^{13}N dissociation, and the extracted $E1$ radiative width was consistent with the one obtained from direct measurements of the $^{12}\text{C}(p,\gamma)^{13}\text{N}$ reaction. However, these agreements are confirmed at accuracies of about 30%. The new experiment was aimed at improving the experimental accuracy to test the Coulomb dissociation method in higher precision.

The experiments were performed at RIKEN using radioactive beams of ^{13}N and ^{14}O with the energies of 76 MeV/nucleon and 85 MeV/nucleon, respectively. The thickness of the Pb target (55 mg/cm 2) was about seven times as thin as that used in the previous experiment at RIKEN [9]. This reduced multiple scattering of the

products in the target, and hence improved the angular resolution. Outgoing charged particles were detected in coincidence by a system similar to the one used for the ^8B Coulomb dissociation experiments at RIKEN.

We observed prominent peaks in the p- ^{12}C and p- ^{13}N relative-energy spectra at around 500 keV corresponding to the $E1$ resonances in ^{13}N and ^{14}O , respectively. The widths (FWHM) of the peaks were 310 keV (^{14}O) and 250 keV (^{13}N), which are better by a factor of two than those in the previous experiment at RIKEN [9]. This is because of the better angular and energy resolutions of the present measurement. The expected accuracy of the yield is in the order of 10%, which allows one to make a precise comparison with the direct-capture results. A preliminary result on the ^{13}N dissociation agree well with the direct (p, γ) result, suggesting reliability of the Coulomb dissociation method.

5 Summary

Several radiative-capture processes in steady and explosive hydrogen burning were studied by the method employing Coulomb excitation to particle-unbound states, namely Coulomb dissociation using radioactive ion beams.

Coulomb dissociation of ^8B was studied at two different energies, 50 and 250 MeV/nucleon. Resultant astrophysical S_{17} -factors are consistent with a recent recommendation $S_{17}(0) = 19_{-2}^{+4}$ eV b [21] obtained by evaluating direct-capture data. This confirms the $^7\text{Be}(p,\gamma)^8\text{B}$ cross-sections used in solar models predicting the neutrino flux. More accurate determination requires further studies on the reaction mechanism of the Coulomb dissociation. Influence of the sub-threshold $3/2^+$ state in ^{15}O to the low-energy $^{14}\text{N}(p,\gamma)^{15}\text{O}$ cross-sections was examined by the Coulomb excitation experiment with a radioactive ^{15}O beam. The results suggest negligible effects of the state to the CNO cycle burning. The hot pp chain is an explosive burning process involving short-lived nuclei. The $^{11}\text{C}(p,\gamma)^{12}\text{N}$ and $^{12}\text{N}(p,\gamma)^{13}\text{O}$ reactions in the chain were studied by the Coulomb dissociation method. New information was extracted from these experiments demonstrating the usefulness of the method for such short-lived nuclei. The ^{13}N Coulomb dissociation result was compared with the direct-capture data for $^{12}\text{C}(p,\gamma)^{13}\text{N}$. The agreement was within 10% showing the reliability of the Coulomb dissociation method.

As discussed above, the Coulomb dissociation method and the spectroscopy by Coulomb excitation are useful for investigating astrophysical capture processes in steady and explosive hydrogen burning. Application of the method to various astrophysical reactions may clarify the role of unstable nuclei for hydrogen burning in various astrophysical sites. Further studies on the reaction mechanism is also required for more accurate determination of the cross-section. Together with the ‘‘ANC’’ method [61] and the direct capture with low-energy RI beams, Coulomb dissociation studies may extend the domain of nuclear astrophysics to the region of nuclei far from the stability line.

References

1. G. Baur, C.A. Bertulani, H. Rebel, Nucl. Phys. A **458**, 188 (1986).
2. G. Baur, H. Rebel, J. Phys. G **20**, 1 (1994); Annu. Rev. Nucl. Part. Sci. **46**, 321 (1996).
3. A.C. Shotter *et al.*, J. Phys. G: Nucl. Phys. **14** (1988) L169
4. H. Utsunomiya *et al.*, Phys. Lett. B **211**, 24 (1988); Nucl. Phys. A **511**, 379 (1990); Phys. Rev. Lett. **65**, 847 (1990).
5. J. Hesselbarth, S. Khan, Th. Kim, K.T. Knöpfle, Z. Phys. A **331**, 365 (1988); J. Hesselbarth, K.T. Knöpfle, Phys. Rev. Lett. **67**, 2773 (1991).
6. J. Kiener, H.J. Gils, H. Rebel, G. Baur, Z. Phys. A **332**, 359 (1989); J. Kiener *et al.*, Phys. Rev. C **44**, 2195 (1991).
7. S.B. Gazes, J.E. Mason, R.B. Roberts, S.G. Teichmann, Phys. Rev. Lett. **68**, 150 (1992); J.E. Mason, S.B. Gazes, R.B. Roberts, S.G. Teichmann, Phys. Rev. C **45**, 2870 (1992).
8. H. Utsunomiya *et al.*, Phys. Lett. B **416**, 43 (1998); Y. Tokimoto *et al.*, Phys. Rev. C **63**, 035801 (2001).
9. T. Motobayashi *et al.*, Phys. Lett. B **264**, 259 (1991).
10. J. Kiener *et al.*, Nucl. Phys. A **552**, 66 (1993).
11. A. Lefebvre *et al.*, Nucl. Phys. A **592**, 69 (1995).
12. T. Motobayashi *et al.*, Phys. Rev. Lett. **73**, 2680 (1994).
13. N. Iwasa *et al.*, J. Phys. Soc. Jpn. **65**, 1256 (1996).
14. T. Kikuchi *et al.*, Phys. Lett. B **391**, 261 (1997).
15. T. Kikuchi *et al.*, Eur. Phys. J. A **3**, 209 (1998).
16. N. Iwasa *et al.*, Phys. Rev. Lett. **83**, 2910 (1999).
17. J. Schwarzenberg *et al.*, Phys. Rev. C **53** (1996) R2598.
18. B. Davids *et al.*, Phys. Rev. Lett. **86**, 2750 (2001).
19. R. Davis Jr., D.S. Harmer, K.C. Hoffman, Phys. Rev. Lett. **20**, 1205 (1968).
20. K. Lande, *Proceedings of the XIX International Conference on Neutrino Physics and Astrophysics, Sudbury, Canada, June 2000*, Nucl. Phys. B **91**, 50 (2001).
21. J.N. Bahcall, M.H. Pinsonneault, S. Basu, *Astrophys. J.* **555**, 990 (2002), preprint (LANL e-print Archive, astro-ph/0010346).
22. Y. Suzuki, *Proceedings of the XIX International Conference on Neutrino Physics and Astrophysics, Sudbury, Canada, June 2000*, Nucl. Phys. B **91**, 29 (2001).
23. SAGE Collaboration (V. Gavrin), *Proceedings of the XIX International Conference on Neutrino Physics and Astrophysics, Sudbury, Canada, June 2000*, Nucl. Phys. B **91**, 36 (2001).
24. GALLEX Collaboration (W. Hampel *et al.*), Phys. Lett. B **447**, 127 (1999).
25. GNO Collaboration (E. Bellotti *et al.*), *Proceedings of the XIX International Conference on Neutrino Physics and Astrophysics, Sudbury, Canada, June 2000*, Nucl. Phys. B **91**, 44 (2001).
26. S.P. Mikheyev, A.Y. Smirnov, *Sov. J. Nucl. Phys.* **42**, 913 (1985); L. Wolfenstein, *Phys. Rev. D* **17**, 2369 (1978).
27. R.W. Kavanagh, *Nucl. Phys.* **15**, 411 (1960).
28. P.D. Parker, *Phys. Rev.* **150**, 851 (1966).
29. R.W. Kavanagh *et al.*, *Bull. Am. Phys. Soc.* **14**, 1209 (1969); *Cosmology, Fusion and other Matters* (Colorado Association, University Press, Boulder, 1972) p. 169.
30. F.J. Vaughn, R.A. Chalmers, D. Kohler, L.F. Chase, Jr., *Phys. Rev. C* **2**, 1657 (1970).
31. C. Wiezorek, H. Krawinkel, R. Santo, L. Wallek, *Z. Phys. A* **282**, 121 (1977).
32. B. Filippone, S.J. Elwyn, C.N. Davids, D.D. Koetke, *Phys. Rev. Lett.* **50**, 412 (1983); *Phys. Rev. C* **28**, 2222 (1983).
33. F. Hammache *et al.*, *Phys. Rev. Lett.* **80**, 928 (1998).
34. M. Hass *et al.*, *Phys. Lett. B* **462**, 237 (1999).
35. L. Gialanella *et al.*, *Eur. Phys. J. A* **7**, 303 (2000).
36. E.G. Adelberger *et al.*, *Rev. Mod. Phys.* **70**, 1265 (1998).
37. T. Kubo *et al.*, *Nucl. Instrum. Methods B* **70**, 309 (1992).
38. F.C. Barker, R.H. Spear, *Astrophys. J.* **307**, 847 (1986).
39. P. Descouvemont, D. Baye, *Nucl. Phys. A* **567**, 341 (1994).
40. H. Geissel *et al.*, *Nucl. Instrum. Methods B* **70**, 286 (1992) (1992)
41. P. Senger *et al.*, *Nucl. Instrum. Methods A* **327**, 393 (1993).
42. B. Davids *et al.*, *Phys. Rev. Lett.* **81**, 2209 (1998).
43. C.A. Bertulani, *Phys. Rev. C* **49**, 2688 (1994).
44. S. Typel, G. Baur, *Phys. Rev. C* **49**, 379 (1994).
45. S. Typel, G. Baur, *Phys. Rev. C* **50**, 2104 (1995).
46. H. Esbensen, G.G. Bertsch, C.A. Bertulani, *Nucl. Phys. A* **581**, 107 (1995).
47. T. Kido, K. Yabana, Y. Suzuki, *Phys. Rev. C* **50** (1994) R1276.
48. C.A. Bertulani, L.F. Canto, M.S. Hussein, *Phys. Lett. B* **353**, 413 (1995).
49. V. Guimarães *et al.*, *Phys. Rev. Lett.* **84**, 1862 (2000).
50. J. Kolata *et al.*, *Phys. Rev. C* **63**, 024616 (2001).
51. F.M. Nunes, I.J. Thompson, *Phys. Rev. C* **59**, 2652 (1999).
52. H. Esbensen, G.F. Bertsch, *Phys. Rev. C* **59**, 3240 (1999).
53. R. Shyam, I.J. Thompson, A.K. Dutt-Mazumder, *Phys. Lett. B* **371**, 1 (1996).
54. U. Schröder *et al.*, *Nucl. Phys. A* **467**, 240 (1987).
55. R. Moreh *et al.*, *Phys. Rev. C* **23**, 988 (1981).
56. A. Jorissen, M. Arnould, *Astron. Astrophys.* **221**, 116 (1989).
57. M. Wiescher *et al.*, *Astrophys. J.* **343**, 352 (1989).
58. P. Descouvemont, I. Baraffe, *Nucl. Phys. A* **514**, 66 (1990).
59. H. Sagawa, Toshio Suzuki, H. Iwasaki, M. Ishihara, *Phys. Rev. C* **63**, 034310 (2001).
60. P. Decrock *et al.*, *Phys. Rev. Lett.* **67**, 808 (1991).
61. H.M. Xu *et al.*, *Phys. Rev. Lett.* **73**, 2027 (1994); A.M. Mukhamedzhanov *et al.*, *Phys. Rev. C* **56**, 1302 (1995).